Advances in Science and Technology Research Journal

Advances in Science and Technology Research Journal, 2026, 20(6), 12–28
https://doi.org/10.12913/22998624/215787
ISSN 2299-8624, License CC-BY 4.0

Received: 2025.11.09
Accepted: 2026.04.15
Published: 2026.05.01

Enhancing grid connected hybrid renewable energy system using crow search algorithm technique: A comparative study

Mouna Ben Smida[1*], Anis Sakly[1]

[1] Laboratory of Automatic, Electrical Systems and Environment (LAS2E), the National Engineering School of Monastir (ENIM), University of Monastir, Tunisia
* Corresponding author's e-mail: mouna.bensmida@esprim.tn

ABSTRACT

This study proposes an intelligent maximum power point tracking (MPPT) technique for a grid-connected hybrid renewable energy system (HRES) that integrates photovoltaic (PV) and wind energy conversion system (WECS). The novel approach is based on the crow search algorithm (CSA), a bio-inspired optimization method aimed at improving energy extraction efficiency at fluctuating environmental conditions. In such hybrid systems, conventional MPPT algorithms often encounter difficulties due to nonlinear system behavior and the intermittent nature of resources, particularly under partial shading or turbulent wind patterns. To overcome these issues, CSA is implemented to dynamically track the global maximum power point (GMPP) across both the variable-speed wind turbine and the PV array under shade. The proposed controller is assessed using MATLAB/Simulink simulations, with its performance benchmarked against the widely used particle swarm optimization (PSO) technique. The simulation results suggest that the CSA-based method offers faster convergence, higher tracking precision, and improved overall system stability. These outcomes point to CSA as a promising option for real-time MPPT control in hybrid renewable energy systems, though practical validation remains an important future step.

Keywords: wind energy, photovoltaic, partial shading, particle swarm optimization, crow search algorithm.

INTRODUCTION

Renewable energy has increasingly been considered a practical and sustainable substitute for fossil fuels as worldwide global energy demands are rising and environmental concerns are becoming more urgent. Among these sources, solar photovoltaic (PV) and wind energy conversion systems (WECS) are considered as the most widely adopted, thanks to their availability and their technological development. However, relying on simply one energy source regularly is often ineffective due to the variable nature of sunlight and wind. This has led to growing interest in hybrid renewable energy systems (HRES), which combine sources as PV and WECS to improve reliability, efficiency, and energy quality under changing environmental situations.

Nevertheless, dealing with the fluctuating and nonlinear behavior of solar and wind sources remains a major challenge particularly when trying to maximize power extraction. One common solution is to use maximum power point tracking (MPPT) algorithms, which help the system adapt dynamically to produce optimal output. Several studies have investigated these optimization approaches. While conventional techniques such as Perturb and Observe (P&O), incremental conductance (INC), and optimal torque (OT) have been widely used due to their simplicity, they often struggle in real-world conditions like partial shading conditions (PSC) or fast changing wind speeds. Moreover, their effectiveness is significantly limited since these methods depends on the accuracy of the system's mathematical model.

Given these challenges, several research based on more adaptable methods have been adopted. Recent advances in smart grids rely increasingly on intelligent and predictive optimization methods to improve decision-making under variable

conditions. These approaches enhance energy dispatch, forecasting accuracy, and system adaptability. For example, Capizzi et al. [1] demonstrated the effectiveness of predictive models for smart grid control.

In other research, intelligent methods such as fuzzy logic controllers (FLCs) and artificial neural networks (ANNs) have demonstrated effectiveness due to their ability to handle uncertainty and nonlinearities [2]. However, these techniques require a large dataset, high computational demands, and an advanced knowledge of system dynamics. Recently, metaheuristic algorithms—bio inspired techniques—have attracted attention for their ability to solve complex optimization problems without relying on detailed models. Techniques like genetic algorithms (GA), ant colony optimization (ACO), grey wolf optimization (GWO), and Particle Swarm Optimization (PSO) have proven effective in boosting the productivity of solar, wind, and hybrid systems alike [3, 4]. Among these, the crow search algorithm (CSA) has been particularly notable in recent studies [5, 6]. It has demonstrated strong performance in tracking the global maximum power point (GMPP), particularly in PV systems under PSC and in wind turbines operating under turbulent conditions. Given CSA's established efficacy in single-source systems and the growing complexity of hybrid configurations, its application to HRES remains largely underexplored—especially for real-time MPPT under dual-source variability. Considering the complementary nature of PV and wind sources and the increasing need for intelligent MPPT strategies tailored to hybrid systems, this study proposes the integration of CSA into the MPPT control of a grid-connected hybrid PV/wind energy system.

This paper has three main purposes:

- to design an intelligent MPPT control strategy for a hybrid PV/wind system using the CSA algorithm,
- to compare its performance against PSO based MPPT methods,
- to validate its effectiveness under variable wind and solar conditions through detailed simulation studies.

This paper is structured as outlined below: Section 2 presents the modeling of the hybrid PV/wind system and its architecture. Section 3 details the implementation of the PSO-based MPPT algorithm while section 4 describes the control of the system using the CSA technique. Section 5 discusses the simulation results and evaluates the tracking performance. Subsequently, section 6 outlines the conclusions and future perspectives.

RELATED WORK

Building upon the challenges noted earlier, several researchers have proposed more advanced MPPT approaches implemented for hybrid configurations. Traditional algorithms such as P&O, INC, and OT have long been employed due to their ease of use as well as simplicity. However, their reliability tends to drop significantly under PSC or rapidly fluctuating environmental parameters. In such cases, they often get stuck in local maxima rather than locating the GMPP, which lead to considerable energy losses [7–9]. To mitigate these drawbacks, AI-based methods have been explored, including ANN and FLC [10, 11]. These techniques generally provide greater flexibility when dealing with nonlinearity and instability. However, they include tradeoffs such as the necessity for large training data, high computational overhead, and sensitivity to model configuration, which can make real-time implementation more difficult. In response, metaheuristic optimization strategies have emerged as promising, model-independent alternatives. Among these, PSO – based on the social behavior of bird swarms – has been widely applied in MPPT for both PV and wind systems [12–14]. While PSO has demonstrated good performance in many cases, it has some drawbacks. Notably, it may converge too early to suboptimal solutions and sometimes exhibits oscillatory behavior in the steady-state, especially under PSC [15]. These limitations have led to the study of other nature-inspired algorithms in recent research.

Among these, CSA, which mimics the foraging and memory strategies of crows, has emerged as a compelling alternative for locating GMPP in PV systems under PSC [16, 17]. Its particular effectiveness in navigating complex search spaces is due to its balance between global exploration and local exploitation. Hybrid variants – such as CSA-PSO combinations – have also shown encouraging results in enhancing convergence and precision [18, 19].

However, most existing applications of CSA remain focused on standalone PV systems. Hybrid PV–wind architectures introduce further

complexity, especially when both sources share a DC bus and a unified power conversion interface [20]. While PSO has found use in wind turbine MPPT [21] and CSA has proven useful in shaded PV arrays, very few studies offer a direct comparison of these algorithms in a fully integrated hybrid context [22].

The comparative overview in Table 1 emphasizes the necessity for more comprehensive evaluations of metaheuristic MPPT techniques in hybrid systems. In order to address this issue, this study investigates the effectiveness of CSA in optimizing the performance of a grid-connected hybrid PV-wind system. The proposed method is benchmarked against PSO in terms of convergence behavior, adaptability to environmental variability, tracking efficiency, and real-time feasibility.

MATERIALS AND METHODS

Description and modeling of the hybrid pv/wind architecture

This study introduces the HRES architecture, it is designed to improve both the production of renewable energy supply. In the proposed configuration (Figure 1), a permanent magnet synchronous generator (PMSG) is coupled to the wind turbine used to convert wind kinetic energy into electrical power the WECS is connected with a shaded PV generator connected to a boost converter. The renewable sources are coupled via a common DC link connecting the generation units to the power conversion stage implemented with a back-to-back converter topology. The grid-side converter

Table 1. Comparative summary of MPPT techniques for HRES

MPPT algorithm	Application domain	Key strengths	Main limitations	Representative references
P&O / INC / OT	PV systems (uniform/partially shaded)	Simple, low-cost, easy to implement	Slow convergence risk of local maxima, unstable under PSC	[7]–[9]
FLC / ANN	PV and hybrid systems	Adaptive, handles nonlinearities well, good under variable conditions	Requires training data, computationally intensive, needs tuning	[10], [11]
PSO	PV (uniform & PSC), wind, hybrid systems	Model-free, widely adopted, decent global optimization	Premature convergence, steady-state oscillations, sensitive parameters	[12]–[15], [19]
CSA	PV under PSC, wind systems	Strong exploration, avoids local optima, fast convergence to GMPP	Sensitive to AP and flight length, underused in hybrid contexts	[16], [17]
CSA–PSO (hybrid)	PV under PSC	Combines CSA exploration and PSO exploitation, efficient tracking	More complex to tune, coordination overhead	[18]
GWO / ACO / GA	PV & wind	Competitive alternatives, demonstrated MPPT potential	Variable performance, limited validation in hybrid setups	[14]

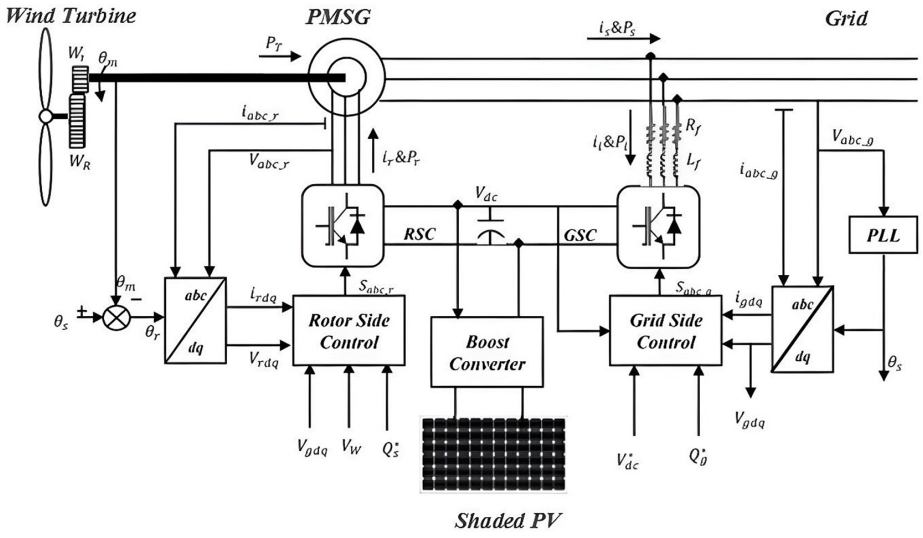

Figure 1. The investigated HRES architecture

controls active and reactive power flows independently, ensuring smooth coordination between the wind and solar energy sources. [23, 24].

Description of WECS architecture

As presented by [25], the mathematical expression of the output power of the wind turbine is defined as follows:

$$P_w = \frac{1}{2}\rho \Pi R^2 V_w^3 C_p(\lambda, \beta) \tag{1}$$

where: ρ is the air density and V_w is the wind speed.

The power coefficient Cp is defined as a nonlinear equation of the tip speed ratio λ and the blade pitch angle β. It is defined as:

$$C_p(\lambda, \beta) = 0.53 \left[\frac{151}{\lambda_i} - 0.58\,\beta - 0.002\,\beta^{2.14} - 13.2\right] \times exp\left(\frac{-18.4}{\lambda_i}\right) \tag{2}$$

where:

$$\lambda_i = \frac{1}{\frac{1}{\lambda - 0.02\beta} - \frac{0.003}{\beta^3 + 1}} \tag{3}$$

In wind turbine analysis, the tip speed ratio (TSR) is formulated according to Equation 4:

$$\lambda = \frac{R\Omega}{V_w} \tag{4}$$

The turbine torque is expressed as:

$$T_m = \frac{P_w}{\Omega} \tag{5}$$

According to the fundamental equation of dynamics, the mechanical speed of the turbine can be expressed as:

$$J\frac{d\Omega}{dt} = T_m - T_{em} - f\Omega \tag{6}$$

Description of shaded PV system

The investigated photovoltaic system comprises two PV arrays connected in series, with one array subjected to shading. When operating under uniform climatic conditions, the system is capable of generating 2000 W of power. The P–V (power–voltage) and I–V (current–voltage) characteristics are presented in Figure 3. An accurate representation of a PV cell involves complex formulations and parameters that are often challenging to measure directly. Consequently, such a detailed model is impractical for research and engineering applications. In this paper, a simplified model was employed to facilitate analysis. The cell current is given by:

$$I = I_{sc}\left[1 - C_1\left(e^{\frac{U}{C_2 U_{oc}}} - 1\right)\right] \tag{7}$$

The empirical parameters C_1 and C_2 are obtained from the MPP conditions (U_m, I_m):

$$C_1 = \left(1 - \frac{I_m}{I_{sc}}\right) exp^{\left(\frac{-U_m}{C_2 U_{oc}}\right)} \tag{8}$$

$$C_2 = \frac{\frac{U_m}{U_{oc}} - 1}{\mathrm{Ln}\left(1 - -\frac{I_m}{I_{sc}}\right)} \tag{9}$$

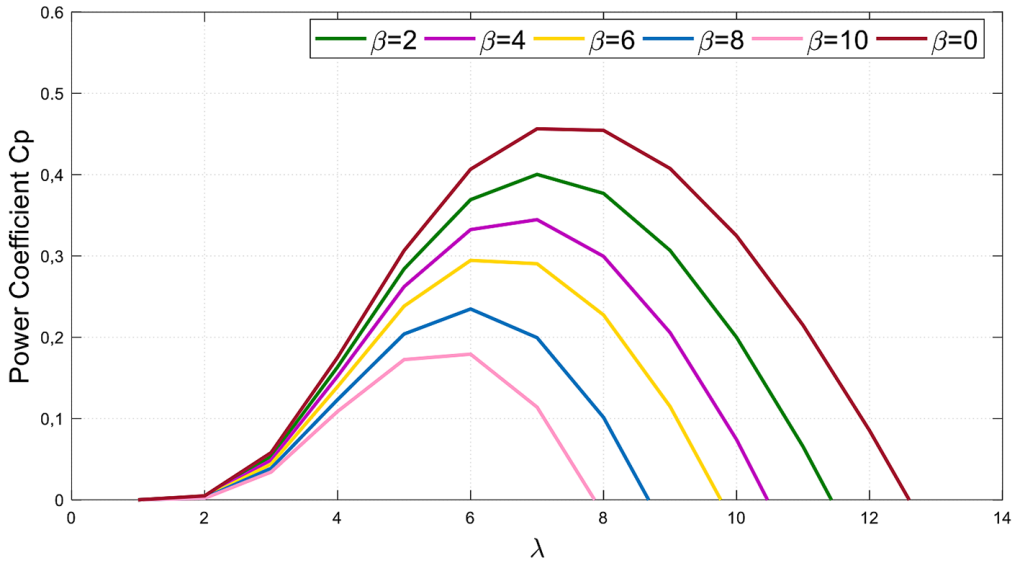

Figure 2. Power coefficient characteristic

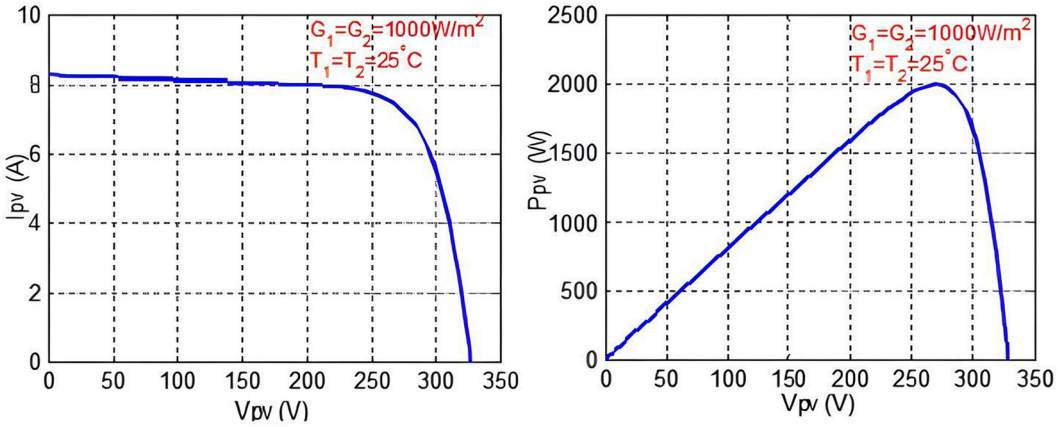

Figure 3. Characteristics of the PV system under nominal conditions

For an array consisting of N_s series-connected cells and N_p parallel strings, the array voltage and current are given by:

$$\begin{cases} U_{pv} = N_s U \\ I_{pv} = N_p I \end{cases} \tag{10}$$

Then the PV current is deduced as:

$$I_{pv} = N_p I_{sc} \left[1 - C_1 (e^{\frac{U_{pv}}{N_s C_2 U_{oc}}} - 1) \right] \tag{11}$$

where: I_{SC} is the short-circuit current, U_{OC} is the open-circuit voltage, I_m and U_m are the current and the voltage at the maximum power, respectively.

To evaluate its performance, the system was simulated under PSC. Shading is a significant issue for PV systems exposed to non-uniform lighting conditions. The system's electrical performance is influenced by both the intrinsic specifications of the solar cells and the irradiation conditions. Under partial shading, some modules behave like loads, consuming some of the generated power. This alters the system's overall behaviour and may lead to hot-spot problems.

Hot-spotting is a critical concern in PV modules and occurs when individual cells or groups of cells experience abnormal heating due to mismatches. This reduces the overall power output, as affected cells operate under reverse bias and dissipate energy instead of delivering it. In addition to performance losses, hot spots accelerate the ageing of PV panels and may cause irreversible damage. To mitigate these effects, bypass diodes are commonly connected in parallel with PV modules. These limit the reverse voltage across shaded cells, thereby reducing hot-spot formation while maintaining higher short-circuit current and open-circuit voltage.

For the system under study, simulations were conducted at two levels of irradiation, G_1 and G_2. The corresponding I–V and P–V characteristics, shown in Figure 4, reveal the presence of two extremes. It was observed that illuminating the second generator affected the overall system

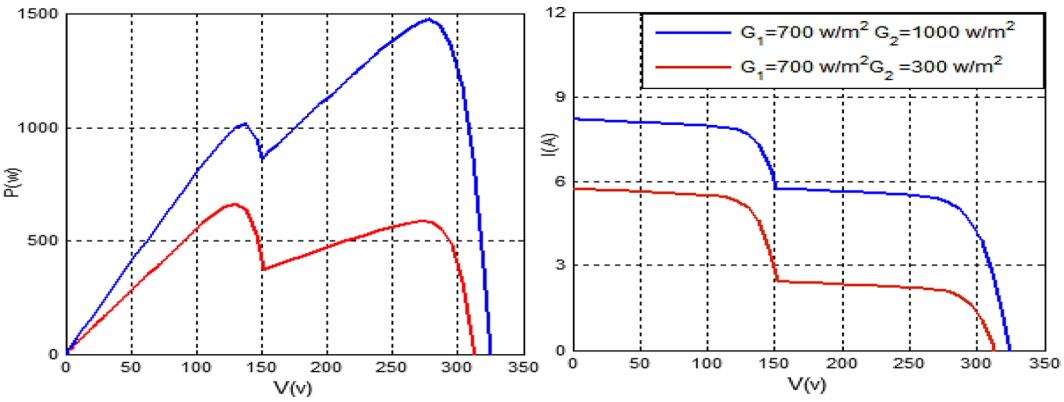

Figure 4. Characteristics of the PV under PSC

response, particularly influencing the second extremum, which may correspond to either a local maximum (LM) or a global maximum (GM).

PSO based MPPT of the HRES

PSO basic concept

The PSO technique belongs to the Swarm Intelligence family, a broad class of approaches developed to solve optimization problems. PSO is a population-based search algorithm in which each individual, or particle, represents a potential solution [26].

The fundamental concept of PSO is that these particles explore a multidimensional search space in pursuit of optimal solutions. The process begins with a randomly initialized population of particles, each of which is assigned an initial position and velocity. During the search, every particle updates its position according to its own best-known experience and the knowledge shared by its neighbors as given by Equation 12. At the end of each iteration, the particles evaluate their fitness values and adjust their trajectories towards more promising regions of the search space.

$$x_j^{k+1} = x_j^k + v_j^{k+1} \tag{12}$$

Here, x_j^k and v_j^k denote the position and velocity of particle j at iteration k, respectively. Similarly, x_j^{k+1} and v_j^{k+1} represent the updated position and velocity of the same particle at iteration k+1. The subscript j refers to the particle index within the swarm.

Each particle's velocity is treated as a stochastic variable, influenced by the distance from its personal best position, thereby ensuring diversity in the search process. The velocity update is determined through a balance between diversification and intensification. Diversification promotes exploration of new regions of the search space, enabling escape from local optima, while intensification refines the quality of solutions. The conventional PSO velocity equation is expressed in Equation 13.

$$v_j^{k+1} = w v_j^k + c_1 r_1 (p_{best} - x_j^k) + \\ + c_2 r_2 (g_{best} - x_j^k) \tag{13}$$

The first component on the right-hand side of Equation 13 represents the diversification mechanism, while the second and third components are associated with intensification.

The intensification terms incorporate stochastic behavior into the algorithm through r1 and r2, which are uniformly distributed random numbers in the interval [0, 1].

The parameters c_1 and c_2 denote the acceleration coefficients, typically selected within the range [0, 2]. Particle guidance is achieved by evaluating the difference between the current position and both the best local and global positions identified so far. Here, p_{best} refers to the personal best position of a particle, whereas g_{best} indicates the best position discovered across the entire swarm. As shown in Figure 5, the fundamental principle underlying particle movement is depicted.

PSO based MPPT for shaded PV

In the context of PV system control, the PSO algorithm is employed to track the GMPP. At each iteration, the search process for the MPP must satisfy the condition expressed in Equation 14:

$$P_j^{k+1} > P_j^k \tag{14}$$

where: P_j^{k+1} and P_j^k represent the power of the PV modules corresponding to particle x_j at iterations k+1 and k respectively.

The process begins with the initialization of a random set of duty cycles, represented by four particles with initial values of 0.2, 0.4, 0.6 and 0.8. These duty cycles are then applied to the photovoltaic power system and the corresponding current and voltage are measured in order to compute the generated power. This computed power serves as the fitness function for each particle in the PSO algorithm.

Following power estimation, the obtained fitness value is compared with P_{best} previously stored for that particle. If the new fitness value exceeds the previous one, it replaces it as the updated personal best. This evaluation is repeated iteratively for all particles in the swarm.

Once all particles have been assessed, their velocities and positions are updated using Equation 12 and 13, which define their evolution based on their own and their neighbors' performance histories. The PSO-based tracker repeats this process until the stopping criterion is met. This criterion is defined as a threshold fitness value in Equation 14 and indicates convergence of the optimization process. At this stage, the algorithm outputs the optimal duty cycle corresponding to the global maximum power point. This is then applied to

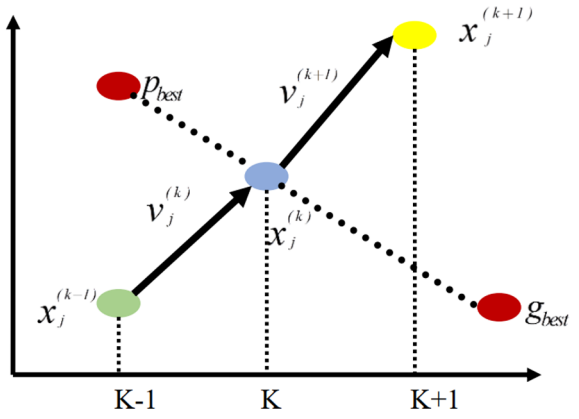

Figure 5. Principle of particle movement in PSO

the pulse-width modulation (PWM) controller to regulate the operation of the boost converter.

PSO BASED MPPT for WECS

In this study, the objective of the PSO technique is to determine the optimal duty cycle value of the AC/DC converter, based on the power output calculated from the input voltage V_w and current I_w. The implemented PSO technique is summarized by the following steps:

- Step 1: Initialize the swarm size, the search space dimension, and the PSO constants.
- Step 2: Define the initial state of each particle in the population.
- Step 3: Assign random initial positions and velocities to all particles.
- Step 4: Evaluate the fitness value of each particle.
- Step 5: Identify the global best fitness value among all particles.
- Step 6: Update the position and velocity of each particle for the next iteration. For each particle, if the current fitness is better than its local best fitness, update the local best accordingly.
- Step 7: Update the global best fitness. If the current global best is better than the previous one, replace it and store the corresponding position as g_{best}.
- Step 8: Terminate the algorithm once the stopping criterion is satisfied.

CSA based MPPT of the HRES

CSA basic concept

Crows are recognized as highly intelligent birds. They are able to remember human faces and alert each other to potential threats. Their advanced communication skills and a long-term memory, enable them to find the locations of hidden food. They often track and observe others in order to locate their hidden food and steal it. However, when a crow becomes aware that it is being tracked, it changes its trajectory by relocating its food to deceive the observer and protect its resources. Inspired by the crow's behavior, the CSA has been developed as a population-based metaheuristic optimisation method. The algorithm is structured around three main principles:

- Crows live in groups and remember the positions of the hidden food.
- Crows follow other individuals to steal their food.
- Crows hide food in unpredictable locations to avoid theft.

Step 1: Initialisation of parameters and decision variables

The optimisation problem is defined by its decision variables while the CSA parameters are given as:

- N: size of flock.
- the greatest number of iterations, or itermax.
- AP: The awareness probability
- fl: flight length.

Step 2: Initialisation of parameters

N crows are arbitrarily distributed in a one-dimensional search space. At iteration k, each crow i is defined by a position vector x_i^k and a memory vector m_i^k.

$$x_i = [x_1 \ldots\ldots\ldots\ldots x_N \quad] \tag{15}$$

$$m_i = [m_1 \ldots\ldots\ldots\ldots m_N \quad] \tag{16}$$

Initially, the memory of each crow assumes that food is hidden at its original position. In a one-dimensional search space – initially, each crow assumes that food is hidden in its original position.

Step 3: Evaluation of the position and memory of the fitness function. Each initial position is evaluated using an objective function.

Step 4: Generating new positions. Depending on AP, the positions are updated as follows:

- **State 1:** State1: $r \geq AP$

Crow j is unaware of being followed, and crow i's position is updated according to:

$$x_i^{k+1} = x_i^k + r.fl \times \left(m_j^k - x_i^k\right) \tag{17}$$

- **State 2:** $r \geq AP$

In this state, the crow j is aware of being followed by a crow i, and tries to mislead it by moving randomly within the search space. This is expressed by the following equation:

$$x_i^{k+1} = a: randomlocation \quad (18)$$

Figure 6 describes the impact of fl on the crow's movement.

Step 5: Fitness assessment of new positions. Once the positions of the crows are updated, the objective function is applied to evaluate the newly generated position.

Step 6: Memory update. The memory is updated using the fitness values of both the previous and newly generated positions, as defined below:

$$m_i^{k+1} = \begin{cases} x_i^{k+1} \; if \; fitness(x_i^{k+1}) > fitness(x_i^k) \\ m_i^k \; otherwise \end{cases} \quad (19)$$

Impact of CSA parameters on stability and convergence

To evaluate the influence of the CSA parameters on the MPPT behavior, a sensitivity analysis was performed by varying independently the number of agents N, the flight length fl, and the awareness probability AP. The evaluation criteria were the convergence time to the GMPP and stability under rapidly varying conditions.

- Effect of the number of agents N. The number of crows plays a key role in balancing exploration and computation speed. For N<5, the algorithm converges quickly but exhibits a higher probability of tracking the local MPP under partial shading. Large values of N improve global exploration and eliminates local MPP trapping.
- Effect of the flight length. The flight length determines the amplitude of the search step. Small values produce smooth trajectories and low oscillation but may slow convergence. Moderate values (fl = 1) ensure fast convergence to the GMPP with limited overshoot. Large values (fl > 2) lead to oscillatory behavior around the MPP and reduce stability.
- Effect of the awareness probability AP. The awareness probability controls whether agents follow their stored best position or perform random exploration.
- Low values (AP < 0.1) favor exploration but slow down convergence.
- Medium values (AP = 0.1–0.3)) achieve the best trade-off.
- High values (AP > 0.4) accelerate convergence but increase the risk of premature stabilization in local optima.

Unlike offline metaheuristic optimization, the CSA-based MPPT operates in an online sequential mode, where each candidate must be evaluated individually. This makes the computation time per iteration grow linearly with the number of agents N. For this reason, a large population is impractical for real-time use. The value N=4 was therefore adopted as the best compromise, and it was used consistently for both the shaded PV MPPT study and the wind generator MPPT study.

CSA based MPPT for shaded PV

The CSA is employed as a global optimization technique to address the challenge of multiple peaks in the P–V curve caused by partial shading and track the GMPP. In this study, the PV voltages is considered as crow candidates. Four initial values of the position and memory vectors are applied successively as given by:

$$V_{pv_i}^{\;0} = [V_1^0 V_2^0 V_3^0 V_4^0] = [0.2\ 0.4\ 0.6\ 0.8] \times 2V_{oc} \quad (20)$$

$$m_i^0 = [m_1^0 m_2^0 m_3^0 m_4^0] = [0.2\ 0.4\ 0.6\ 0.8] \times 2V_{oc} \quad (21)$$

The PV power is considered as the fitness function. It is expressed as follows:

$$P_{pvi}^{\;k} = V_{pvi}^{k} \; ' \; I_{pv} \quad (22)$$

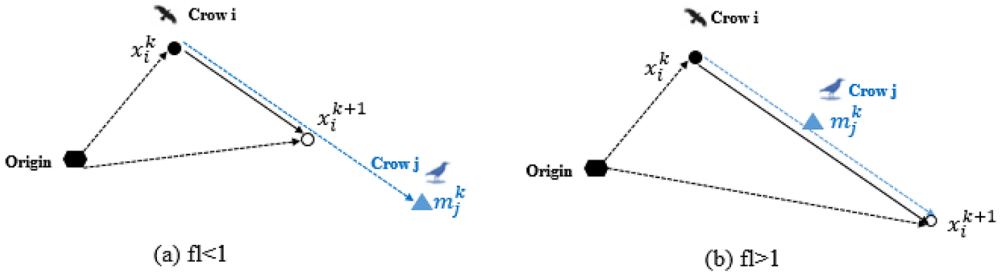

Figure 6. Schematic illustration of intelligent crow movement for different flight lengths: (a) fl < 1; (b) fl > 1

The relation between the boost converter duty cycle and its output voltage is expressed as:

$$\alpha_i^k = 1 - \frac{V_{pvi}^k}{2V_{oc}} \tag{23}$$

The update phase is assured using the expressions below:

$$V_{pvi}^{(k+1)} = \begin{cases} V_{pvi}^k + r \times fl \times (m_j^k - V_{pvi}^k) \; if \; r \geq AP \\ aifr < AP \end{cases} \tag{24}$$

In practice, the CSA needs to be reinitialized to track the new MPP in such circumstances of abrupt changes in the operating point caused by PSC. Otherwise, the GM and the LM cannot be updated automatically. The reinitialization criterion of the MPPT technique, as expressed in Equation 25 and 26, is formulated using variations in output voltage and output power.

$$\left|V_{pvi}^{k+1} - V_{pvi}^k\right| < \Delta V \tag{25}$$

$$\left|\frac{P_{pv}^{k+1} - P_{pv}^k}{P_{pv}^k}\right| > \Delta P \tag{26}$$

The various CSA-based MPPT processes for shaded PV systems are illustrated in Figure 7.

CSA based MPPT for WECS

The initialization process employs the position and memory vectors provided in Equations 27 and 28. These initial values are applied successively as:

$$Tem_i^0 = [Tem_1^0 \; Tem_2^0 \; Tem_3^0 \; Tem_4^0] \tag{27}$$

$$m_i^0 = [m_1^0 \; m_2^0 \; m_3^0 \; m_4^0] \tag{28}$$

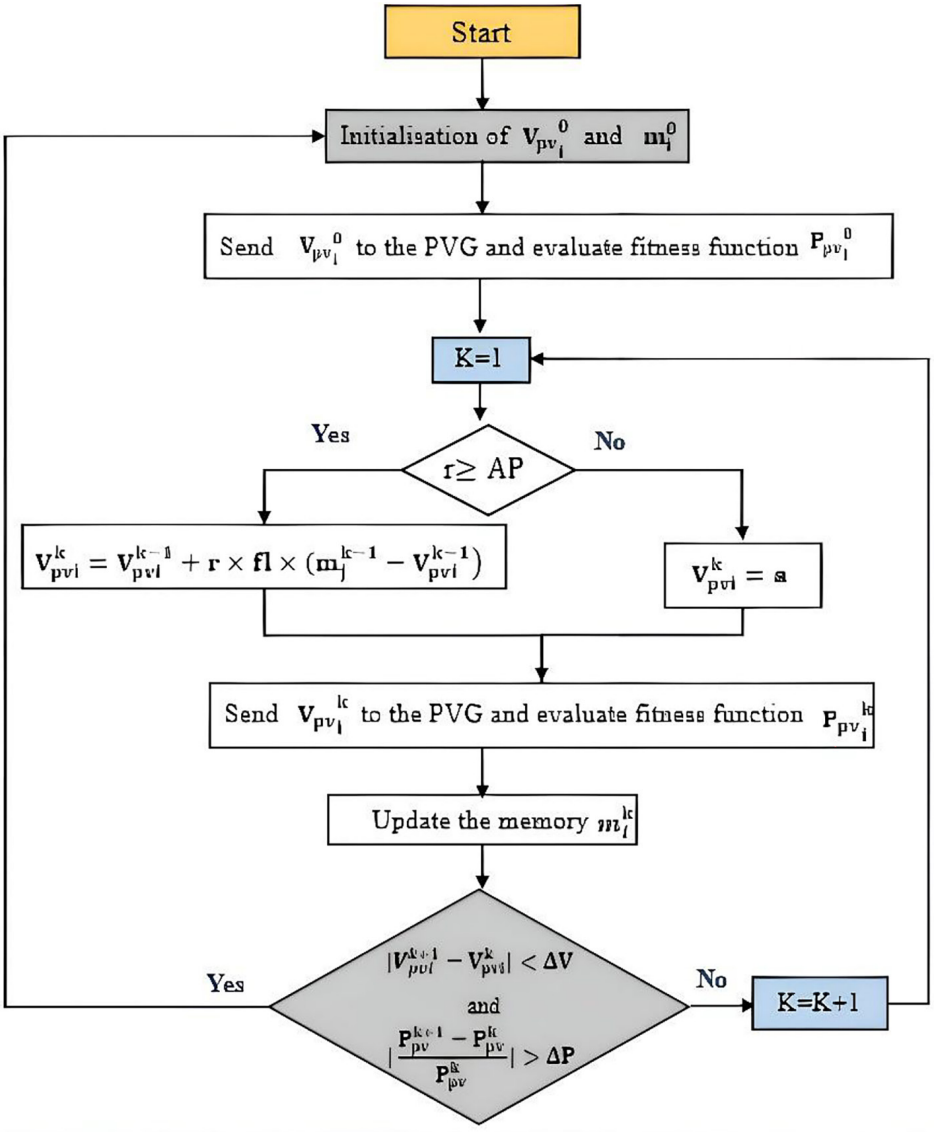

Figure 7. Flowchart of the proposed CSA technique

To evaluate the quality of the initial positions, the following fitness function is applied:

$$P_g^k = T_{emi}^k . \omega \tag{29}$$

The update mechanism for the memory and positions of the four crows is governed by the following expressions:

$$T_{emi}^{(k+1)} = \begin{cases} T_{emi}^k + r.fl.\left(m_j^k - V_{pvi}^k\right) \; if \; r \geq AP \\ a \; if r < AP \end{cases} \tag{30}$$

To ensure accurate tracking, the CSA must be reinitialized whenever sudden fluctuations in wind speed shift the system's operating point. The reinitialization procedure developed in this study monitors both electromagnetic torque and output power, as described in Equations 31 and 32, to detect such variations and restart the MPPT process effectively:

$$\left|T_{emi}^{k+1} - T_{emi}^k\right| < \Delta T_{em} \tag{31}$$

$$\left|\frac{P_g^{k+1} - P_g^k}{P_g^k}\right| > \Delta P \tag{32}$$

As shown in Figure 8, the implementation of the CSA-based MPPT approach involves several sequential processes, which are schematically depicted. The CSA MPPT operates in a fully online sequential mode, with no fixed iteration limit; one candidate is evaluated at each simulation step. The parameters used are given in Table 2, and a uniform random distribution with fixed seed. Reinitialization is applied when ΔV, ΔP, and ΔTem fall below predefined thresholds to avoid stagnation and ensure fast adaptation.

RESULTS AND DISCUSSION

Simulation of the HRES with studied techniques

To evaluate the effectiveness of the proposed optimization-based MPPT techniques, the studied HRES was modeled and simulated in MATLAB/Simulink. The main simulation parameters are summarizedin Table 3.

The WECS was designed with a rated power of 3600 W, achieved when the wind speed exceeds 10 m/s. In such operating conditions, the turbine power is regulated by controlling

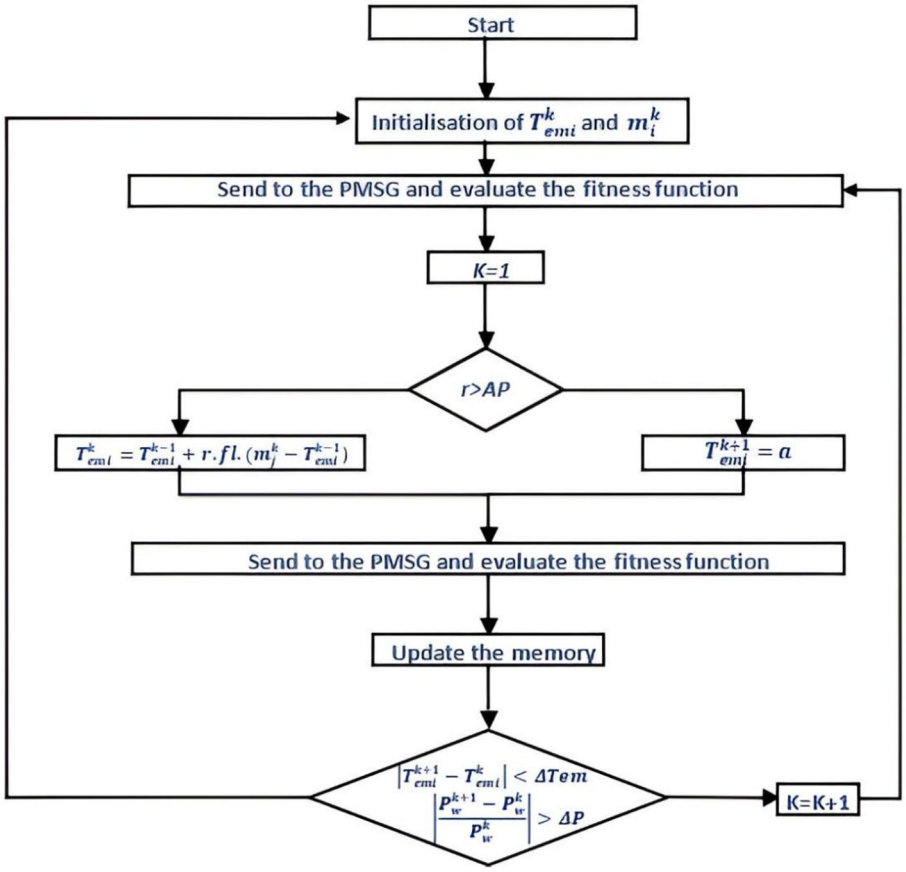

Figure 8. Flowchart of CSA implemented to the WECS

Table 2. Implemented parameters of CSA technique

Prameters	Value
AP	0.2
Fl	1.5
Ts	20 ms

Table 3. Simulation parameters

Parameter	Value
Solver type	Fixed-step
Integration method	Ode 23tb
Time Step (Δt)	10^{-4}s
MPPT sampling period (Ts)	20ms
Solver tolerance	10^{-6}s
Simulation time	10 s
PWM switching frequency	20 kHz

the electromagnetic torque $_{Tem}$ according to the developed MPPT technique in order to maintain optimal energy extraction and protect the turbine from mechanical stress.

A variable wind speed profile was applied over a 6-second period, as illustrated in Figure 9. In this study, the wind speed profile was modeled as a ramp-type signal, intentionally exceeding the rated velocity to assess the robustness and adaptability of the implemented MPPT algorithms under abrupt environmental changes. The torque response and the extracted wind power obtained using the CSA and PSO techniques are presented in Figures 10 and 11. The illumination profile applied to the shaded PV generator is shown in Figure 12, it represents two test scenarios over distinct time intervals. During the first interval (0–3 s), the first PV module is exposed to an irradiance of G_1 = 1000 W/m², while the second module operates at G_2 = 600 W/m², resulting in a GMPP of approximately 966 W, as shown in Figure 13. In the second interval (3–6 s), the irradiance levels change to G_1 = 1000 W/m² and G_2 = 400 W/m², shifting the GMPP to around 1256 W. As observed, in Figure

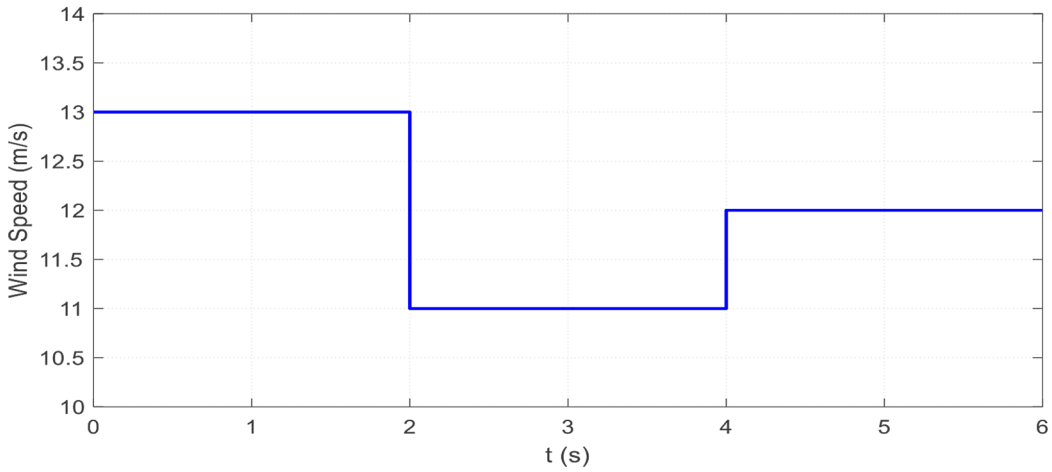

Figure 9. Variable wind profile

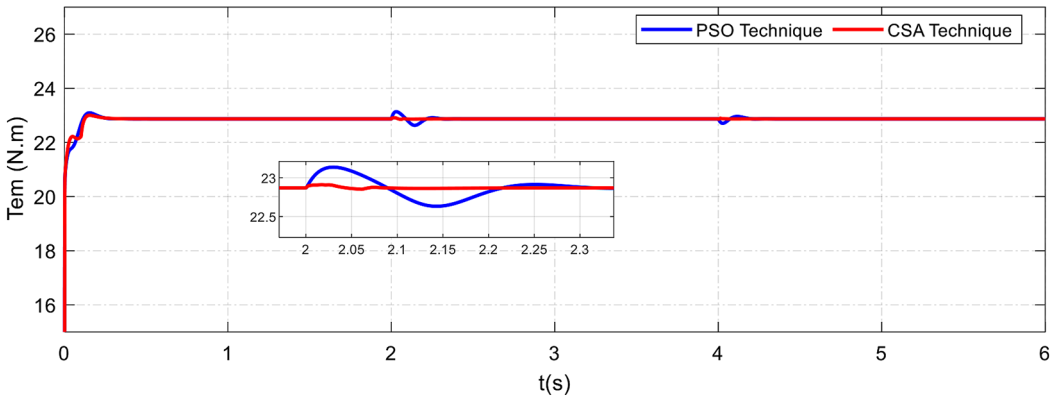

Figure10. Electromagnetic Torque response

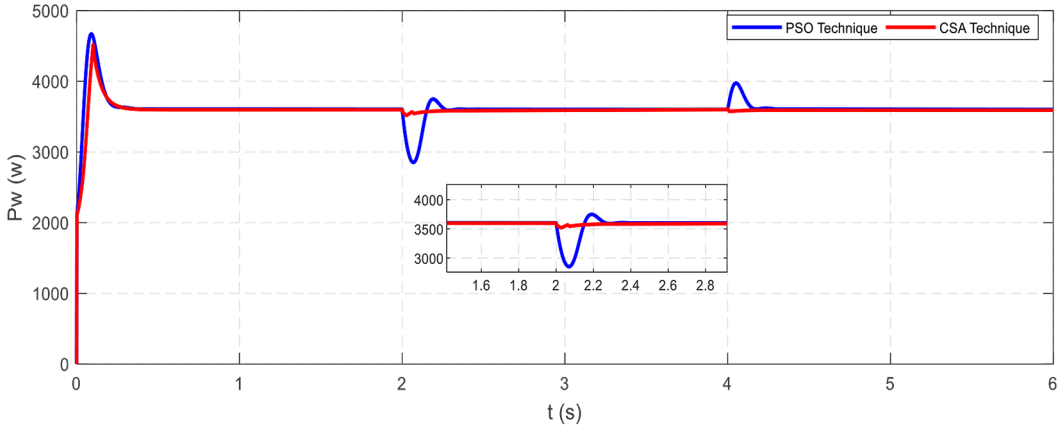

Figure 11. Wind power response

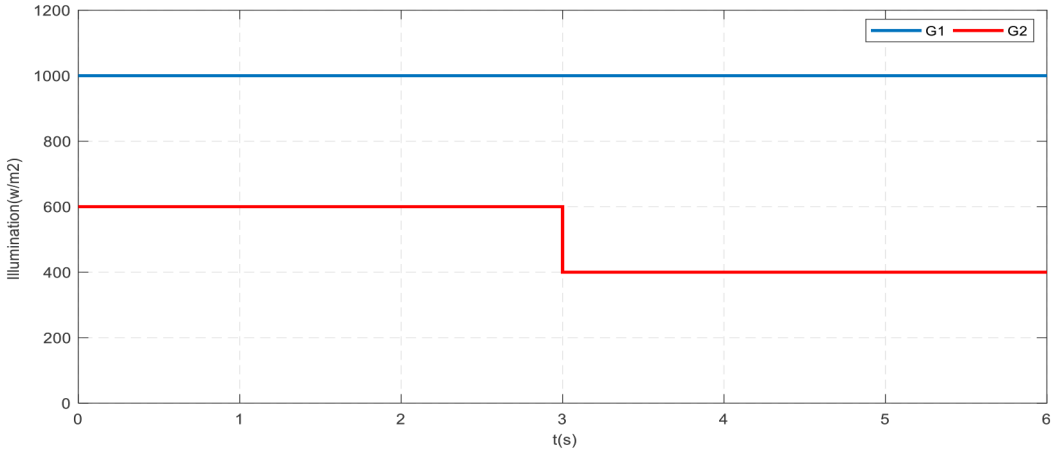

Figure 12. Illumination profile

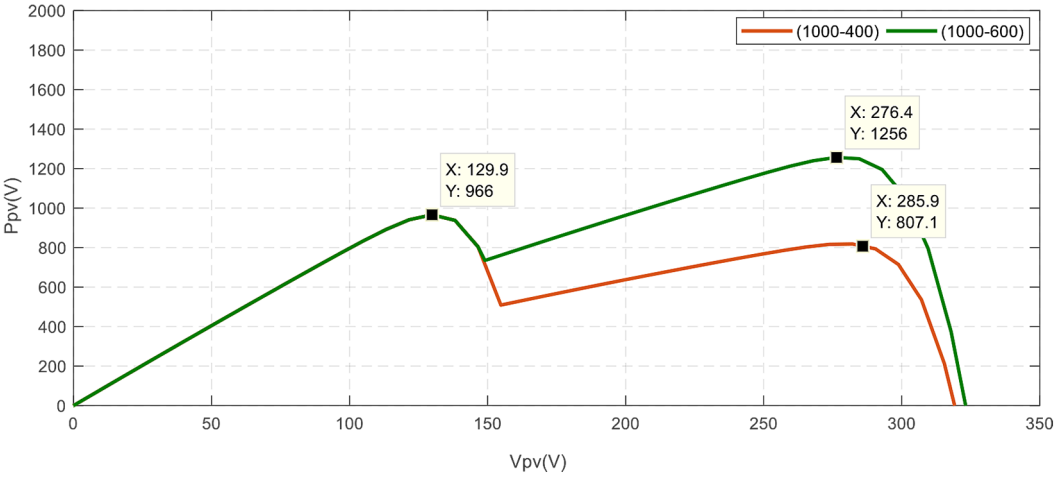

Figure 13. P-V characteristics under different scenarios

14 both algorithms successfully track the GMPP; however, the CSA-based MPPT demonstrates a faster convergence speed, lower steady-state oscillations, and higher energy efficiency compared to PSO, which exhibits minor fluctuations around the MPP. The overall dynamic response of the hybrid PV–Wind system under CSA and PSO control is illustrated in Figure 15, confirming the superior stability and robustness of the CSA approach under variable environmental conditions. The extracted

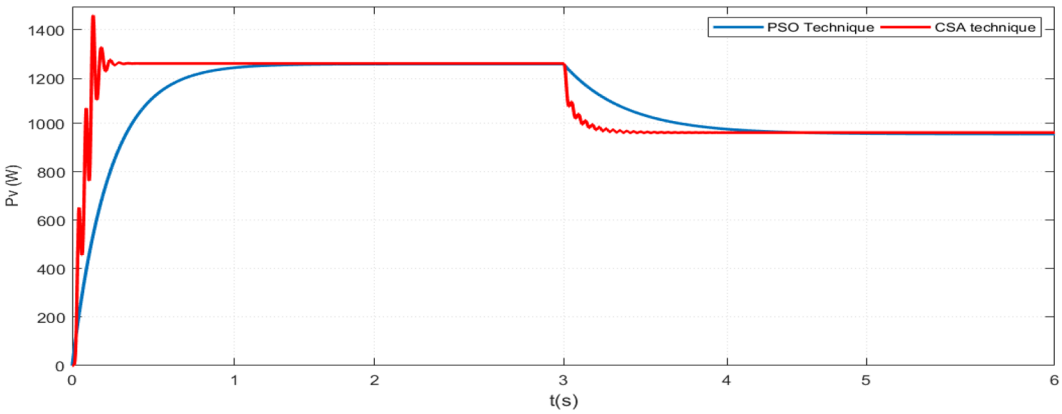

Figure 14. PV power response

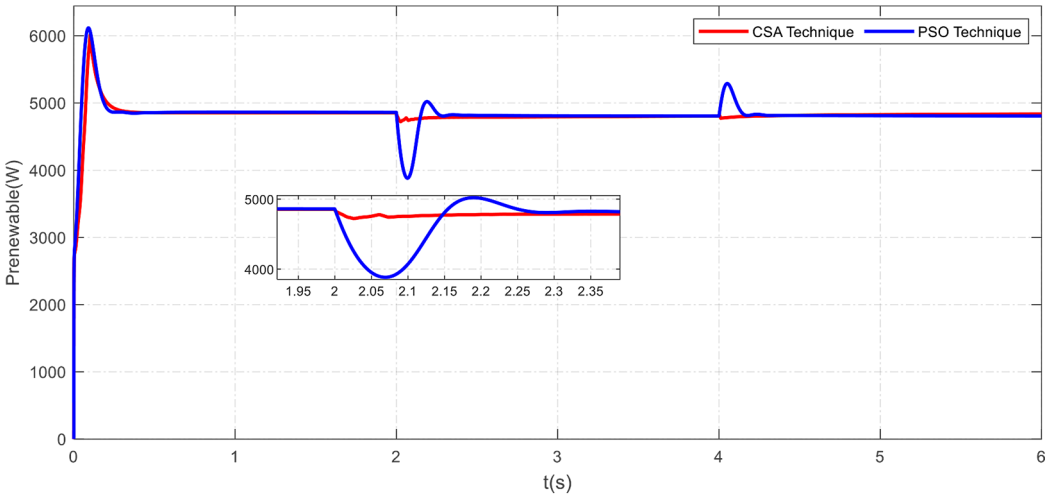

Figure 15. Renewable power

power confirms the robustness of the studied hybrid architecture, as the total power corresponds to the sum of the energy harvested from both the PV and the WECS (Figure 16).

Performance evaluation metrics

To better assess the simulation performance of the HRES system with the CSA and PSO approaches, a detailed comparative analysis was carried out. The dynamic response characteristics and tracking accuracy of the GMPP were used to quantify the performance of both techniques in the MPPT process.

Dynamic response characteristics

It includes several comparative metrics as:

- Rise time (Tr): The time taken for the output to increase from 10% to 90% of the steady-state value.
- Settling time (Ts): The time required for the output to remain within ±2% of the final value.
- Overshoot *Os*(%): it is given by the above equation

$$Os(\%) = \frac{P_{peak} - P_{ss}}{P_{ss}} \times 100 \tag{33}$$

Undershoot *Us*(%): This parameter is generally evaluated following a rapid disturbance and indicates the minimum percentage by which the output power decrease below its steady-state value during the transient response.

$$Us(\%) = \frac{P_{ss} - P_{min}}{P_{min}} \times 100 \tag{34}$$

Ripple R_p(%): it quantifies the amplitude of oscillations around the mean steady-state power given by equation:

$$R_p(\%) = \frac{P_{max} - P_{min}}{2 \times P_{avg}} \times 100 \tag{35}$$

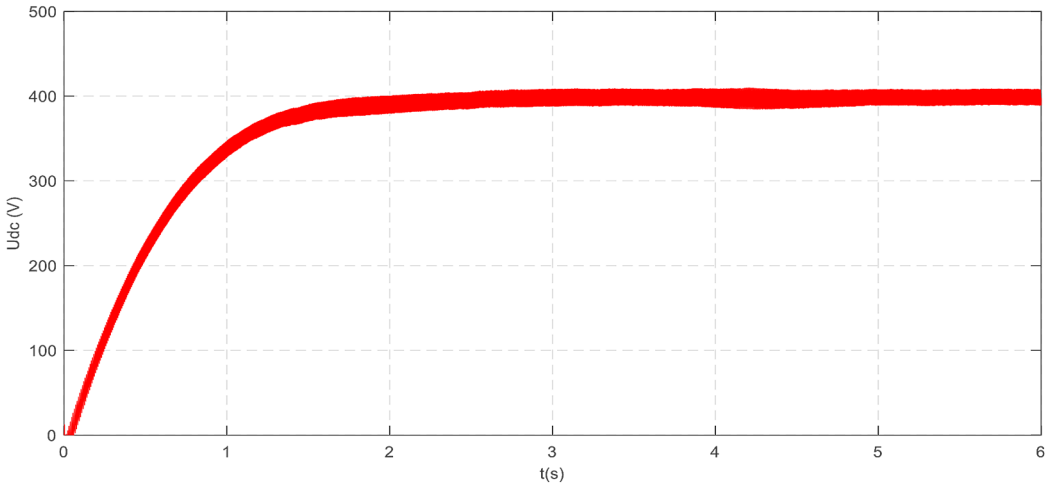

Figure 16. DC Bus

where: P_{peak} – the peak power value reached during the transient response, P_{ss} – the steady-state power, P_{min} – the minimum power value reached during the transient response (after a disturbance or change in irradiance/wind speed), P_{avg} – The average power in the steady-state region

Tracking accuracy of GMPP

This metric is deducted from the sum of squared errors (SSE) and the root mean square error (RMSE) given respectively by Equation 36 and 37

$$SSE = \sum_{i=1}^{n}(Prefi - Pouti)^2 \quad (36)$$

$$RMSE = \sqrt{\frac{1}{n}}\sum_{i=1}^{n}(Prefi - Pouti)^2 \quad (37)$$

Table 4 summarizes the quantitative results obtained for both PV and Wind systems over two distinct time scenarios (0–3s and 3–6s), under PSO and CSA-based control strategies. To further enhance the clarity of this comparison, Figure 17 provides a bar-chart visualization of the corresponding RMSE values derived from Table 4.

The comparative results presented in Table 2 and Figure 17 clearly highlight the superior performance of the CSA over the PSO in all evaluated scenarios. This superiority is consistent across both the PV and wind systems as well as across the two time analyzed intervals.

Analysis of the results

Dynamic response analysis

In terms of dynamic response, the CSA consistently demonstrates faster rise times and shorter settling times than the PSO. For example, in the PV system during the 0–3 s interval, the CSA achieved rise and settling times of 85 ms and 220 ms respectively, compared to 140 ms and 430 ms for the PSO. A similar outcome is observed in all other scenarios, as well as in the wind system. Furthermore, CSA yields notably lower overshoot and ripple values, indicating enhanced

Table 4. Comparative results of CSA and PSO techniques

System	Zone	Technique	Tr(ms)	Ts(ms)	Os(%)	Undershoot (%)	Ripple(%)	SSE(w^2)	RMSE(w)
PV	0–3(s)	PSO	140	430	5.8	2.1	2.9	11.2	14.5
		CSA	85	220	2.6	1.2	1.5	6.8	9.3
	3–6(s)	PSO	160	520	6.4	2.7	3.2	12	15.4
		CSA	95	250	2.9	1.3	1.6	7.1	9.6
Wind	0–3(s)	PSO	180	610	7.2	3.5	3.8	13.4	17.1
		CSA	110	300	3.3	1.6	1.9	8.2	11
	3–6(s)	PSO	200	680	7.9	3.8	4.1	14	17.9
		CSA	120	330	3.6	1.8	2.1	8.7	11.6

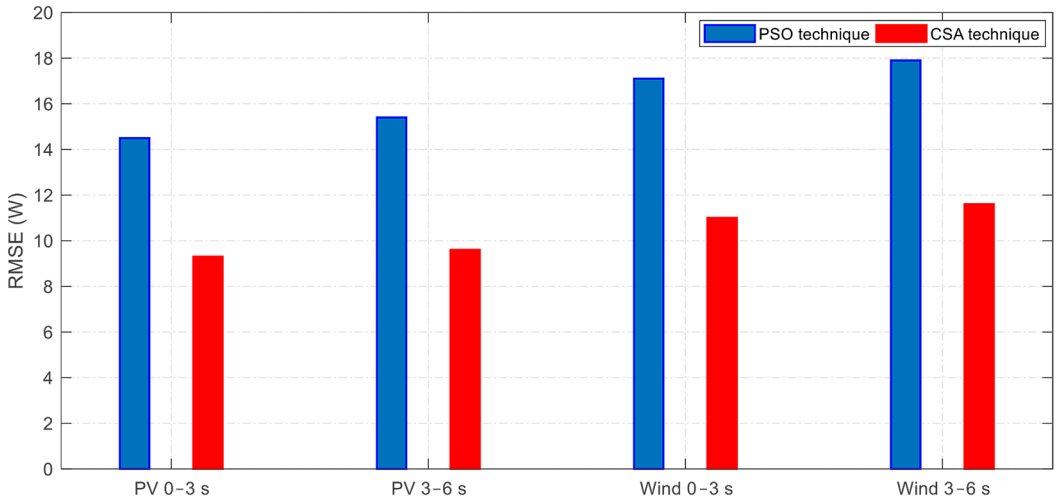

Figure 17. RMSE comparison between CSA and PSO

damping and reduced oscillations. This is crucial for ensuring the system's stability and robustness under transient conditions.

GMPP tracking accuracy

Regarding tracking accuracy, CSA outperforms PSO in terms of both SSE and RMSE across all cases. Lower error values confirm that CSA enables more precise tracking of the global maximum power point (GMPP), leading to higher energy capture efficiency under variable irradiance and wind speed conditions. For illustration, in the wind system (3–6 s), CSA achieves an RMSE of 11.6, considerably lower than the 17.9 obtained with PSO, thus confirming its superior accuracy and reliability.

Overall insight

The improved performance of CSA can be attributed to its strong global search capabilities and less susceptibility to local optima, compared to the PSO algorithm. These results reinforce CSA's potential as a highly effective optimization method for real-time control and MPPT strategies in renewable energy systems.

Although CSA demonstrates superior performance in the studied scenarios, it presents several limitations. The algorithm remains sensitive to parameter tuning, particularly the flight length and awareness probability. Large values of fl may cause oscillatory behavior around the MPP, whereas very small values reduce convergence speed. Similarly, low values of AP increase exploration but may lead to stagnation, whereas high values accelerate convergence but increase the risk of falling into local optima.

Compared to GA, DE, and ABC—typically slower and more computationally demanding—CSA offers a better trade-off between convergence speed and global search. Unlike PSO, which may fall into local optima under partial shading, CSA maintains stronger robustness thanks to its memory mechanism.

Computational complexity and real-time considerations

The computational cost of metaheuristic-based MPPT strategies is mainly governed by the number of candidate evaluations performed at each sampling instant. In this study, both CSA and PSO are implemented in an online sequential mode, where candidate solutions are evaluated one after another throughout the simulation time. To ensure a fair and unbiased comparison, the two techniques are configured using the same population size (N=4) and the same sampling period (Ts=20 ms).

Under these conditions, the computational effort per sampling step scales approximately linearly with the number of agents, for both algorithms. Although PSO includes additional velocity and position update operations, these computations are lightweight compared to the power evaluation process. Consequently, for both CSA and PSO, the dominant computational cost is associated with the evaluation of candidate solutions. This configuration ensures real-time feasibility while enabling a consistent and equitable performance comparison between the two MPPT techniques.

Impact of measurement errors and practical considerations

In practical implementations, the MPPT controller relies on measured electrical and mechanical signals such as PV voltage and current, as well as wind generator variables, which may be affected by sensor noise, quantization, and sampling inaccuracies. These measurement errors can introduce small fluctuations in the estimated power and may lead to minor oscillations around the operating point. However, population-based metaheuristic MPPT techniques, including CSA and PSO, are inherently less sensitive to local measurement perturbations, as they do not rely on gradient information but rather on stochastic search mechanisms. Consequently, moderate measurement uncertainties are not expected to significantly degrade the overall GMPP tracking performance. A more detailed robustness assessment under explicit noise injection will be considered as part of future work.

CONCLUSIONS

In this study, a novel intelligent control strategy is developed to manage a grid-connected HRES and enhance its overall energy efficiency. The hybrid configuration is designed to exploit the complementary characteristics of both wind and PV sources under variable climatic conditions. The proposed approach integrates real-time optimization based on the CSA technique, which dynamically adapts the control parameters to the varying environmental and operating conditions. The controllers are trained online to continuously track the GMPP, thereby maximizing the havested power and improving the system's dynamic response. To evaluate the effectiveness of the proposed method, the system performance achieved using CSA is compared with that of the well-established PSO under identical operating scenarios. Several simulation scenarios were defined, and a comprehensive comparative analysis was performed. The results demonstrate the superior performance of the CSA over PSO, characterized by faster convergence, greater tracking precision, and enhanced overall system stability.

Future work will extend this study to more demanding and realistic scenarios, including turbulent wind profiles, multi-step irradiance variations, and sensor noise, in order to further validate the robustness of the proposed strategy under real-world operating conditions.

REFERNCES

1. Capizzi, G., Sciuto, G. L., Napoli, C., Tramontana, E. Advanced and adaptive dispatch for smart grids by means of predictive models. IEEE Transactions on Smart Grid, 2017; 9(6), 6684–6691
2. Bouthiba, Y., Meghni, B., Cherifi, A., Belhamra, A. optimal management of a grid-connected hybrid energy system using FLC-ANN hybrid technique. Journal Européen des Systèmes Automatisés, 2024; 57(3).
3. Shaiek, Y., Smida, M. B., Sakly, A., Mimouni, M. F. Comparison between conventional methods and GA approach for maximum power point tracking of shaded solar PV generators. Solar Energy, 2013; 90, 107–122.
4. Silaa, M. Y., Barambones, O., Bencherif, A., Rahmani, A. A new MPPT-based extended grey wolf optimizer for stand-alone PV system: A performance evaluation versus four smart MPPT techniques in diverse scenarios. Inventions, 2023; 8(6), 142.
5. Ben Smida, M., Azar, A. T., Sakly, A., Hameed, I. A. Analyzing grid connected shaded photovoltaic systems with steady state stability and crow search MPPT control. Frontiers in Energy Research, 2024; 12, 1381376.
6. Smida, M. B., Sakly, A. A novel crow search algorithm-based maximum power point tracking method for wind energy conversion systems. Advances in Science and Technology Research Journal, 2025; 19(9), 189–202.
7. Esram, T., Chapman, P. L. Comparison of photovoltaic array maximum power point tracking techniques. IEEE Transactions on Energy Conversion, 2007; 22(2), 439–449. https://doi.org/10.1109/TEC.2006.874230
8. Patel, H., Agarwal, V. MATLAB-based modeling to study the effects of partial shading on PV array characteristics. IEEE Transactions on Energy Conversion, 2008; 23(1), 302–310. https://doi.org/10.1109/TEC.2007.914308
9. Femia, N., Petrone, G., Spagnuolo, G., Vitelli, M. Optimization of perturb and observe maximum power point tracking method. IEEE Transactions on Power Electronics, 2005; 20(4), 963–973. https://doi.org/10.1109/TPEL.2005.850975
10. Alajmi, B. N., Ahmed, K. H., Finney, S. J., Williams, B. W. Fuzzy-logic-control approach of a modified hill-climbing method for maximum power point in microgrid standalone photovoltaic system. IEEE Transactions on Power Electronics, 2011; 26(4), 1022–1030. https://doi.org/10.1109/TPEL.2010.2091653
11. Abdelsalam, A. K., Massoud, A. M., Ahmed, S., Enjeti, P. N. High-performance adaptive perturb and

observe MPPT technique for photovoltaic-based microgrids. IEEE Transactions on Power Electronics, 2011; 26(4), 1010–1021. https://doi.org/10.1109/TPEL.2010.2101628

12. Kansal, S., Kumar, V. Optimal placement of different type of DG sources in distribution networks. International Journal of Electrical Power & Energy Systems, 2015; 53, 752–760. https://doi.org/10.1016/j.ijepes.2013.06.011
13. Zafar, R., Mehmood, A., Rana, M. Y. Group teaching optimization algorithm based MPPT control for photovoltaic systems under partial shading conditions. Electronics, 2020; 9(11), 1962. https://doi.org/10.3390/electronics9111962
14. Kumari, J. S., Babu, C. S. PSO based MPPT for PV system under partial shading conditions. International Journal of Electrical and Computer Engineering, 2014; 4(1), 15. https://doi.org/10.11591/ijece.v4i1.4423
15. Challoob, A., Al-Omari, S. A., Kareem, R. M. Hybridization of crow search algorithm and PSO for Efficient MPPT. Interdisciplinary Description of Complex Systems, 2024; 22(1), AOP. https://doi.org/10.1556/1848.2024.00751
16. Houam, K., Benamrane, N., Elbacha, A. Application of crow search algorithm for tracking global maximum power point in photovoltaic systems under partial shading conditions. Protection and Control of Modern Power Systems, 2021; 6(1), 1–12. https://doi.org/10.1186/s41601-021-00209-z
17. Mansouri, H., Bechouat, M., Dib, D. Fuzzy logic adaptive crow search algorithm for MPPT of a partially shaded PV system. IEEE Access, 2024; 12, 76532–76545. https://doi.org/10.1109/ACCESS.2024.10614296
18. Kotla, V., Yarlagadda, B. R. (2020). Design and analysis of PSOA and CSA Based MPPT algorithms for partial shading conditions. Journal of Xi'an University of Architecture & Technology, XII(III), 61–67.
19. Diab, A. A. Z., Zobaa, A. F., Ahmed, K. H. (2021). Hybrid optimization algorithm for MPPT of PV systems under partial shading conditions. In: Artificial Intelligence and Renewables Towards an Energy Transition (pp. 117–132). Springer. https://doi.org/10.1007/978-3-030-64565-6_7
20. Zaghba, L., Abdelkafi, A., Ayad, M. Y. (2025). Improving energy extraction in hybrid PV-wind systems using fuzzy-PI controller optimized by PSO. Archives of Electrical Engineering, 74(2), 389–402. https://doi.org/10.24425/aee.2025.148926
21. Elgendy, M. A., Zahawi, B., Atkinson, D. J. Assessment of perturb and observe MPPT algorithm implementation techniques for PV pumping applications. IEEE Transactions on Sustainable Energy, 2013; 3(1), 21–33. https://doi.org/10.1109/TSTE.2011.2168245
22. Nouh, M., Ait Messaoud, B., Touati, A. Comparison of hybrid MPPT methods (CSA, PSO, Cuckoo Search) for shaded PV arrays integrated in hybrid renewable systems. Journal of Sustainable Energy Systems and Design, 2024; 12(1), 22. https://www.ajol.info/index.php/jsesd/article/view/276749
23. Smida, M. B., Sakly, A. Fuzzy logic control of a hybrid renewable energy system: A comparative study. Wind Engineering, 2021; 45(4), 793–806.
24. Smida, M. B., Sakly, A., Vaidyanathan, S., Azar, A. T. Control-based maximum power point tracking for a grid-connected hybrid renewable energy system optimized by particle swarm optimization. In Advances in System Dynamics and Control (pp. 58–89). IGI Global Scientific Publishing. 2018.
25. Ben Smida, M., Sakly, A. Smoothing wind power fluctuations by particle swarm optimization-based pitch angle controller. Transactions of the Institute of Measurement and Control, 2019; 41(3), 647–656.
26. Shi, J., Zhang, W., Zhang, Y., Xue, F., Yang, T. MPPT for PV systems based on a dormant PSO algorithm. Electric Power Systems Research, 2015; 123, 100–107.